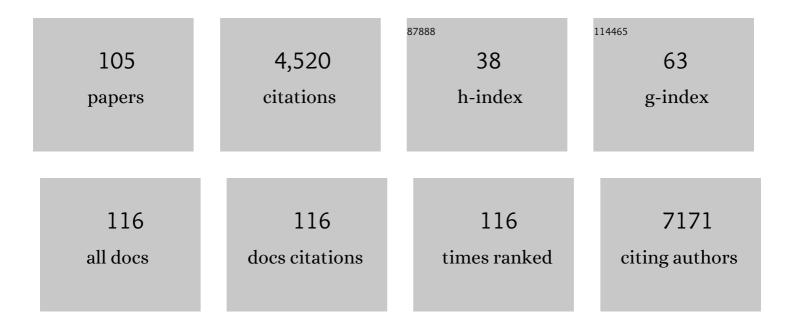
List of Publications by Year in descending order

Source: https://exaly.com/author-pdf/1441387/publications.pdf Version: 2024-02-01



#	Article	IF	CITATIONS
1	Positron Emission Tomography Imaging of Adenoviral-Mediated Transgene Expression in Liver Cancer Patients. Gastroenterology, 2005, 128, 1787-1795.	1.3	211
2	Transplantation of adipose derived stromal cells is associated with functional improvement in a rat model of chronic myocardial infarction. European Journal of Heart Failure, 2008, 10, 454-462.	7.1	188
3	Activation of Human Cerebral and Cerebellar Cortex by Auditory Stimulation at 40 Hz. Journal of Neuroscience, 2002, 22, 10501-10506.	3.6	179
4	The HIF-1α Hypoxia Response in Tumor-Infiltrating T Lymphocytes Induces Functional CD137 (4-1BB) for Immunotherapy. Cancer Discovery, 2012, 2, 608-623.	9.4	156
5	Agonist Anti-CD137 mAb Act on Tumor Endothelial Cells to Enhance Recruitment of Activated T Lymphocytes. Cancer Research, 2011, 71, 801-811.	0.9	137
6	EANM practice guideline/SNMMI procedure standard for dopaminergic imaging in Parkinsonian syndromes 1.0. European Journal of Nuclear Medicine and Molecular Imaging, 2020, 47, 1885-1912.	6.4	134
7	Assessment of biliary bicarbonate secretion in humans by positron emission tomography. Gastroenterology, 1999, 117, 167-172.	1.3	129
8	Increased Oral Bioavailability of Resveratrol by Its Encapsulation in Casein Nanoparticles. International Journal of Molecular Sciences, 2018, 19, 2816.	4.1	118
9	A synthetic peptide from transforming growth factor Î ² type III receptor inhibits liver fibrogenesis in rats with carbon tetrachloride liver injury. Cytokine, 2003, 22, 12-20.	3.2	114
10	Guidance on current good radiopharmacy practice (cGRPP) for the small-scale preparation of radiopharmaceuticals. European Journal of Nuclear Medicine and Molecular Imaging, 2010, 37, 1049-1062.	6.4	113
11	Dendritic cells delivered inside human carcinomas are sequestered by interleukin-8. International Journal of Cancer, 2005, 116, 275-281.	5.1	112
12	Dual Tracer 11C-Choline and FDC-PET in the Diagnosis of Biochemical Prostate Cancer Relapse After Radical Treatment. Molecular Imaging and Biology, 2010, 12, 210-217.	2.6	109
13	A phase I clinical trial of thymidine kinase-based gene therapy in advanced hepatocellular carcinoma. Cancer Gene Therapy, 2010, 17, 837-843.	4.6	103
14	The nigrostriatal system in the presymptomatic and symptomatic stages in the MPTP monkey model: A PET, histological and biochemical study. Neurobiology of Disease, 2012, 48, 79-91.	4.4	93
15	Multipotent adult progenitor cells sustain function of ischemic limbs in mice. Journal of Clinical Investigation, 2008, 118, 505-14.	8.2	93
16	Meox2/Tcf15 Heterodimers Program the Heart Capillary Endothelium for Cardiac Fatty Acid Uptake. Circulation, 2015, 131, 815-826.	1.6	88
17	In vivo study of the mucus-permeating properties of PEC-coated nanoparticles following oral administration. European Journal of Pharmaceutics and Biopharmaceutics, 2015, 97, 280-289.	4.3	87
18	EANM procedure guidelines for brain PET imaging using [18F]FDG, version 3. European Journal of Nuclear Medicine and Molecular Imaging, 2022, 49, 632-651.	6.4	82

#	Article	IF	CITATIONS
19	Zein nanoparticles for oral folic acid delivery. Journal of Drug Delivery Science and Technology, 2015, 30, 450-457.	3.0	77
20	Expression of <i>MALT1</i> oncogene in hematopoietic stem/progenitor cells recapitulates the pathogenesis of human lymphoma in mice. Proceedings of the National Academy of Sciences of the United States of America, 2012, 109, 10534-10539.	7.1	73
21	Quantitative volumetric analysis of gliomas with sequential MRI and 11C-methionine PET assessment: patterns of integration in therapy planning. European Journal of Nuclear Medicine and Molecular Imaging, 2012, 39, 771-781.	6.4	71
22	Transplantation of Mesenchymal Stem Cells Exerts a Greater Long-Term Effect than Bone Marrow Mononuclear Cells in a Chronic Myocardial Infarction Model in Rat. Cell Transplantation, 2010, 19, 313-328.	2.5	70
23	PEG-PGA enveloped octaarginine-peptide nanocomplexes: An oral peptide delivery strategy. Journal of Controlled Release, 2018, 276, 125-139.	9.9	70
24	Bioadhesive properties and biodistribution of cyclodextrin–poly(anhydride) nanoparticles. European Journal of Pharmaceutical Sciences, 2009, 37, 231-240.	4.0	68
25	Progression of dopaminergic depletion in a model of MPTP-induced Parkinsonism in non-human primates. An 18F-DOPA and 11C-DTBZ PET study. Neurobiology of Disease, 2010, 38, 456-463.	4.4	66
26	Impact of Time-of-Flight and Point-Spread-Function in SUV Quantification for Oncological PET. Clinical Nuclear Medicine, 2013, 38, 103-109.	1.3	66
27	Sustained Attention in a Counting Task: Normal Performance and Functional Neuroanatomy. Neurolmage, 2002, 17, 411-420.	4.2	65
28	Voxel-Based Analysis of Dual-Time-Point ¹⁸ F-FDG PET Images for Brain Tumor Identification and Delineation. Journal of Nuclear Medicine, 2011, 52, 865-872.	5.0	65
29	Gene therapy imaging in patients for oncological applications. European Journal of Nuclear Medicine and Molecular Imaging, 2005, 32, S384-S403.	6.4	61
30	Antitumor and antiangiogenic effect of the dual EGFR and HER-2 tyrosine kinase inhibitor lapatinib in a lung cancer model. BMC Cancer, 2010, 10, 188.	2.6	61
31	Pilot Clinical Trial of Type 1 Dendritic Cells Loaded with Autologous Tumor Lysates Combined with GM-CSF, Pegylated IFN, and Cyclophosphamide for Metastatic Cancer Patients. Journal of Immunology, 2011, 187, 6130-6142.	0.8	59
32	Human serum albumin nanoparticles for ocular delivery of bevacizumab. International Journal of Pharmaceutics, 2018, 541, 214-223.	5.2	56
33	Infiltration of plasma rich in growth factors enhances in vivo angiogenesis and improves reperfusion and tissue remodeling after severe hind limb ischemia. Journal of Controlled Release, 2015, 202, 31-39.	9.9	52
34	Functional neuroanatomy of sustained attention in schizophrenia: Contribution of parietal cortices. Human Brain Mapping, 2002, 17, 116-130.	3.6	48
35	Deletion of Inducible Nitric-Oxide Synthase in Leptin-Deficient Mice Improves Brown Adipose Tissue Function. PLoS ONE, 2010, 5, e10962.	2.5	46
36	Automated analysis of FDG PET as a tool for single-subject probabilistic prediction and detection of Alzheimer's disease dementia. European Journal of Nuclear Medicine and Molecular Imaging, 2013, 40, 1394-1405.	6.4	42

#	Article	IF	CITATIONS
37	Decreased carbon-11-flumazenil binding in early Alzheimer's disease. Brain, 2012, 135, 2817-2825.	7.6	41
38	Adipose Stromal Vascular Fraction Improves Cardiac Function in Chronic Myocardial Infarction through Differentiation and Paracrine Activity. Cell Transplantation, 2012, 21, 1023-1037.	2.5	40
39	Role of positron emission tomography in urological oncology. BJU International, 2010, 106, 1578-1593.	2.5	38
40	Cyclodextrin-poly(anhydride) nanoparticles as new vehicles for oral drug delivery. Expert Opinion on Drug Delivery, 2011, 8, 721-734.	5.0	38
41	Conjunctival vaccination against Brucella ovis in mice with mannosylated nanoparticles. Journal of Controlled Release, 2012, 162, 553-560.	9.9	36
42	European regulations for the introduction of novel radiopharmaceuticals in the clinical setting. Quarterly Journal of Nuclear Medicine and Molecular Imaging, 2017, 61, 135-144.	0.7	33
43	Intensive Pharmacological Immunosuppression Allows for Repetitive Liver Gene Transfer With Recombinant Adenovirus in Nonhuman Primates. Molecular Therapy, 2010, 18, 754-765.	8.2	31
44	Molecular Imaging Techniques to Study the Biodistribution of Orally Administered 99mTc-Labelled Naive and Ligand-Tagged Nanoparticles. Molecular Imaging and Biology, 2011, 13, 1215-1223.	2.6	29
45	Statistical parametric maps of 18F-FDG PET and 3-D autoradiography in the rat brain: a cross-validation study. European Journal of Nuclear Medicine and Molecular Imaging, 2011, 38, 2228-2237.	6.4	29
46	Positron emission tomography and gene therapy: basic concepts and experimental approaches for gene expression imaging. Molecular Imaging and Biology, 2004, 6, 225-238.	2.6	28
47	MAPC Transplantation Confers a more Durable Benefit than AC133+ Cell Transplantation in Severe Hind Limb Ischemia. Cell Transplantation, 2011, 20, 259-270.	2.5	28
48	PET optimization for improved assessment and accurate quantification of ⁹⁰ Yâ€microsphere biodistribution after radioembolization. Medical Physics, 2014, 41, 092503.	3.0	28
49	Untangling the web of European regulations for the preparation of unlicensed radiopharmaceuticals. Nuclear Medicine Communications, 2015, 36, 414-422.	1.1	28
50	Preclinical safety of topically administered nanostructured lipid carriers (NLC) for wound healing application: biodistribution and toxicity studies. International Journal of Pharmaceutics, 2019, 569, 118484.	5.2	28
51	Twelve automated thresholding methods for segmentation of PET images: a phantom study. Physics in Medicine and Biology, 2012, 57, 3963-3980.	3.0	27
52	Significant dose reduction is feasible in FDG PET/CT protocols without compromising diagnostic quality. Physica Medica, 2018, 46, 134-139.	0.7	27
53	New MRI, 18F-DOPA and 11C-(+)-α-dihydrotetrabenazine templates for Macaca fascicularis neuroimaging: Advantages to improve PET quantification. NeuroImage, 2009, 47, 533-539.	4.2	24
54	Toxicity Studies of Poly(Anhydride) Nanoparticles as Carriers for Oral Drug Delivery. Pharmaceutical Research, 2012, 29, 2615-2627.	3.5	24

#	Article	IF	CITATIONS
55	Non-invasive in vivo imaging of cardiac stem/progenitor cell biodistribution and retention after intracoronary and intramyocardial delivery in a swine model of chronic ischemia reperfusion injury. Journal of Translational Medicine, 2017, 15, 56.	4.4	24
56	cAMP activates transcription of the human glucocorticoid receptor gene promoter. Journal of Steroid Biochemistry and Molecular Biology, 1998, 67, 89-94.	2.5	23
57	A Fully Automated One Pot Synthesis of 9-(4-[18F]Fluoro-3-Hydroxymethylbutyl) Guanine for Gene Therapy Studies. Molecular Imaging and Biology, 2002, 4, 415-424.	2.6	23
58	Study of the neutron field in the vicinity of an unshielded PET cyclotron. Physics in Medicine and Biology, 2005, 50, 5141-5152.	3.0	23
59	PET Tracers for Clinical Imaging of Breast Cancer. Journal of Oncology, 2012, 2012, 1-9.	1.3	23
60	Simple automated system for simultaneous production of 11C-labeled tracers by solid supported methylation. Applied Radiation and Isotopes, 2006, 64, 808-811.	1.5	22
61	In vivo efficacy of bevacizumab-loaded albumin nanoparticles in the treatment of colorectal cancer. Drug Delivery and Translational Research, 2020, 10, 635-645.	5.8	22
62	Engineering a genomeâ€reduced bacterium to eliminate <i>Staphylococcus aureus</i> biofilms <i>inÂvivo</i> . Molecular Systems Biology, 2021, 17, e10145.	7.2	21
63	13N-Ammonia PET as a Measurement of Hindlimb Perfusion in a Mouse Model of Peripheral Artery Occlusive Disease. Journal of Nuclear Medicine, 2007, 48, 1216-1223.	5.0	20
64	Monoaminergic PET imaging and histopathological correlation in unilateral and bilateral 6-hydroxydopamine lesioned rat models of Parkinson's disease: A longitudinal in-vivo study. Neurobiology of Disease, 2015, 77, 165-172.	4.4	19
65	Glucose metabolism during fasting is altered in experimental porphobilinogen deaminase deficiency. Human Molecular Genetics, 2016, 25, 1318-1327.	2.9	19
66	COVID-19 and the brain: impact on nuclear medicine in neurology. European Journal of Nuclear Medicine and Molecular Imaging, 2020, 47, 2487-2492.	6.4	18
67	Glucocerebrosidase Gene Therapy Induces Alpha-Synuclein Clearance and Neuroprotection of Midbrain Dopaminergic Neurons in Mice and Macaques. International Journal of Molecular Sciences, 2021, 22, 4825.	4.1	18
68	Synthesis of S-[13N]nitrosoglutathione (13N-GSNO) as a new potential PET imaging agent. Applied Radiation and Isotopes, 2009, 67, 95-99.	1.5	17
69	<i>In Vivo</i> Monitoring of Staphylococcus aureus Biofilm Infections and Antimicrobial Therapy by [¹⁸ F]Fluoro-Deoxyglucose–MicroPET in a Mouse Model. Antimicrobial Agents and Chemotherapy, 2014, 58, 6660-6667.	3.2	17
70	Radiopharmaceuticals are special, but is this recognized? The possible impact of the new Clinical Trials Regulation on the preparation of radiopharmaceuticals. European Journal of Nuclear Medicine and Molecular Imaging, 2014, 41, 2005-2007.	6.4	17
71	Mannosylated Nanoparticles for Oral Immunotherapy in a Murine Model of Peanut Allergy. Journal of Pharmaceutical Sciences, 2019, 108, 2421-2429.	3.3	17
72	The effect of thiamine-coating nanoparticles on their biodistribution and fate following oral administration. European Journal of Pharmaceutical Sciences, 2019, 128, 81-90.	4.0	16

#	Article	IF	CITATIONS
73	PET imaging of thymidine kinase gene expression in the liver of non-human primates following systemic delivery of an adenoviral vector. Gene Therapy, 2009, 16, 136-141.	4.5	15
74	Toxicity and biodistribution of orally administered casein nanoparticles. Food and Chemical Toxicology, 2017, 106, 477-486.	3.6	15
75	Adeno-Associated Virus Liver Transduction Efficiency Measured by <i>in Vivo</i> [¹⁸ F]FHBG Positron Emission Tomography Imaging in Rodents and Nonhuman Primates. Human Gene Therapy, 2011, 22, 999-1009.	2.7	14
76	Radiation dosimetry and biodistribution in non-human primates of the sodium/iodide PET ligand [18F]-tetrafluoroborate. EJNMMI Research, 2015, 5, 70.	2.5	14
77	Dissolving Microneedles for Intradermal Vaccination against Shigellosis. Vaccines, 2019, 7, 159.	4.4	14
78	The specific case of radiopharmaceuticals and GMP—activities of the Radiopharmacy Committee. European Journal of Nuclear Medicine and Molecular Imaging, 2008, 35, 1400-1401.	6.4	12
79	Modulation of the fate of zein nanoparticles by their coating with a Gantrez® AN-thiamine polymer conjugate. International Journal of Pharmaceutics: X, 2019, 1, 100006.	1.6	12
80	Effective protection of mice against Shigella flexneri with a new self-adjuvant multicomponent vaccine. Journal of Medical Microbiology, 2017, 66, 946-958.	1.8	12
81	Assessment of metabolic patterns and new antitumoral treatment in osteosarcoma xenograft models by [18F]FDG and sodium [18F]fluoride PET. BMC Cancer, 2018, 18, 1193.	2.6	11
82	The new Regulation on clinical trials in relation to radiopharmaceuticals: when and how will it be implemented?. EJNMMI Radiopharmacy and Chemistry, 2019, 4, 2.	3.9	9
83	[18F]fluorothymidine-positron emission tomography in patients with locally advanced breast cancer under bevacizumab treatment: Usefulness of different quantitative methods of tumor proliferation. Revista Espanola De Medicina Nuclear E Imagen Molecular, 2014, 33, 280-285.	0.0	8
84	Levodopa induces long-lasting modification in the functional activity of the nigrostriatal pathway. Neurobiology of Disease, 2014, 62, 250-259.	4.4	8
85	In vivo SPECT-CT imaging and characterization of technetium-99m-labeled bevacizumab-loaded human serum albumin pegylated nanoparticles. Journal of Drug Delivery Science and Technology, 2021, 64, 101809.	3.0	8
86	mRNA-based therapy in a rabbit model of variegate porphyria offers new insights into the pathogenesis of acute attacks. Molecular Therapy - Nucleic Acids, 2021, 25, 207-219.	5.1	7
87	Design and performance evaluation of single-use whole-sterile "plug & play―kits for routine automated production of [11C]choline and [11C]methionine with radiopharmaceutical quality. Applied Radiation and Isotopes, 2010, 68, 2298-2301.	1.5	6
88	High value of 64Cu as a tool to evaluate the restoration of physiological copper excretion after gene therapy in Wilson's disease. Molecular Therapy - Methods and Clinical Development, 2022, 26, 98-106.	4.1	6
89	Cerebral metabolic pattern associated with progressive parkinsonism in non-human primates reveals early cortical hypometabolism. Neurobiology of Disease, 2022, 167, 105669.	4.4	5
90	Imaging studies for evaluating gene therapy in translational research. Drug Discovery Today: Technologies, 2005, 2, 335-343.	4.0	4

#	Article	IF	CITATIONS
91	Radiation protection in an animal research unit with pet: Occupational doses and dose rates produced by animals. Radiation Measurements, 2011, 46, 1307-1309.	1.4	2
92	Recomendaciones para la nomenclatura de compuestos radiomarcados. Revista Espanola De Medicina Nuclear E Imagen Molecular, 2020, 39, 1-2.	0.0	2
93	Preparación, radiomarcaje con 99mTc y 67Ga y estudios de biodistribución de nanopartÃculas de albúmina con recubrimientos poliméricos. Revista Espanola De Medicina Nuclear E Imagen Molecular, 2020, 39, 225-232.	0.0	2
94	Preclinical safety of negatively charged microspheres (NCMs): Optimization of radiolabeling for in vivo and ex vivo biodistribution studies after topical administration on full-thickness wounds in a rat model. European Journal of Pharmaceutics and Biopharmaceutics, 2022, 177, 61-67.	4.3	2
95	Clinical Applications of Reporter Gene Technology. , 0, , 297-314.		1
96	The Clinical Translation Process in Europe. , 2019, , 607-618.		1
97	Highlight selection of radiochemistry and radiopharmacy developments by editorial board (January–June 2020). EJNMMI Radiopharmacy and Chemistry, 2021, 6, 5.	3.9	1
98	Lessons from 11C-dihydrotetrabenazine imaging in a xenograft mouse model of rat insulinoma: is PET imaging of pancreatic beta cell mass feasible?. Quarterly Journal of Nuclear Medicine and Molecular Imaging, 2017, 61, 447-455.	0.7	1
99	Positron emission tomography (PET) imaging of AdCMVTk biodistributionin ortothopic hepatocellular carcinoma gene therapy. Journal of Hepatology, 2002, 36, 265-266.	3.7	0
100	Spectra and Neutron Dosimetry Inside a PET Cyclotron Vault Room. AIP Conference Proceedings, 2006, , .	0.4	0
101	Radiopharmaceutical Manufacturing. , 0, , 59-96.		0
102	Mapping transplanted endothelial progenitor cells migration after an acute liver injury: A bimodal PET-Luminometry imaging study. Vascular Pharmacology, 2012, 56, 385-386.	2.1	0
103	FRI-430-Preclinical validation of copper 64 as a translational tool for evaluating the pharmacodynamics of VTX-801 genen therapy in Wilson's disease. Journal of Hepatology, 2019, 70, e583.	3.7	0
104	Randomized phase II study with dendritic cell (DC) immunotherapy in patients with resected hepatic metastasis of colorectal carcinoma Journal of Clinical Oncology, 2014, 32, TPS3129-TPS3129.	1.6	0
105	286â€Tumor targeting and tissue biodistribution of RO7122290, a novel FAP-targeted 4–1BB (CD137) agonist, in patients with advanced solid tumors, using [89Zr]-RO7122290 as a PET tracer. , 2020, , .		0